

Syntectonic infiltration by meteoric waters along the Sevier thrust front, southwest Montana

A. C. RYGEL*, D. J. ANASTASIO AND G. E. BEBOUT

Department of Earth and Environmental Sciences, Lehigh University, Bethlehem, PA, USA

ABSTRACT

Structural, petrographic, and isotopic data for calcite veins and carbonate host-rocks from the Sevier thrust front of SW Montana record syntectonic infiltration by H₂O-rich fluids with meteoric oxygen isotope compositions. Multiple generations of calcite veins record protracted fluid flow associated with regional Cretaceous contraction and subsequent Eocene extension. Vein mineralization occurred during single and multiple mineralization events, at times under elevated fluid pressures. Low salinity ($T_m = -0.6^\circ\text{C}$ to $+3.6^\circ\text{C}$, as NaCl equivalent salinities) and low temperature (estimated 50–80°C for Cretaceous veins, 60–80°C for Eocene veins) fluids interacted with wall-rock carbonates at shallow depths (3–4 km in the Cretaceous, 2–3 km in the Eocene) during deformation. Shear and extensional veins of all ages show significant intra- and inter-vein variation in $\delta^{18}\text{O}$ and $\delta^{13}\text{C}$. Carbonate host-rocks have a mean $\delta^{18}\text{O}_{\text{V-SMOW}}$ value of $+22.2 \pm 3\text{‰}$ (1σ), and both the Cretaceous veins and Eocene veins have $\delta^{18}\text{O}$ ranging from values similar to those of the host-rocks to as low as $+5$ to $+6\text{‰}$. The variation in vein $\delta^{13}\text{C}_{\text{V-PDB}}$ of -1 to approximately $+6\text{‰}$ is attributed to original stratigraphic variation and C isotope exchange with hydrocarbons. Using the estimated temperature ranges for vein formation, fluid (as H₂O) $\delta^{18}\text{O}$ calculated from Cretaceous vein compositions for the Tendoy and Four Eyes Canyon thrust sheets are -18.5 to -12.5‰ . For the Eocene veins within the Four Eyes Canyon thrust sheet, calculated H₂O $\delta^{18}\text{O}$ values are -16.3 to -13.5‰ .

Fluid–rock exchange was localized along fractures and was likely coincident with hydrocarbon migration. Paleotemperature determinations and stable isotope data for veins are consistent with the infiltration of the foreland thrust sheets by meteoric waters, throughout both Sevier orogenesis and subsequent orogenic collapse. The cessation of the Sevier orogeny was coincident with an evolving paleogeographic landscape associated with the retreat of the Western Interior Seaway and the emergence of the thrust front and foreland basin. Meteoric waters penetrated the foreland carbonate thrust sheets of the Sevier orogeny utilizing an evolving mesoscopic fracture network, which was kinematically related to regional thrust structures. The uncertainty in the temperature estimates for the Cretaceous and Eocene vein formation prevents a more detailed assessment of the temporal evolution in meteoric water $\delta^{18}\text{O}$ related to changing paleogeography. Meteoric water-influenced $\delta^{18}\text{O}$ values calculated here for Cretaceous to Eocene vein-forming fluids are similar to those previously proposed for surface waters in the Eocene, and those observed for modern-day precipitation, in this part of the Idaho-Montana thrust belt.

3 Key words: xxx, xxx, xxx, xxx, xxx

2 Received Xx Xxxx 200x; accepted Xx Xxxx 200x

Corresponding author: David Anastasio, Department of Earth and Environmental Sciences, 31 Williams Drive, Lehigh University, Bethlehem, PA 18015-3188, USA.

1 Email: dja2@lehigh.edu. Tel: xxx. Fax: xxx.


*Current address: Department of Environmental Quality, Suite 400, 1200 N Street, PO Box 98922, Lincoln, NE 68509, USA.

Geofluids (2006) 6, 1–14

INTRODUCTION

The evolution of orogens and foreland basins is influenced by aqueous fluids, which impact deformation and mass

transport (Hubbert & Rubey 1959; Davis *et al.* 1983; Forster & Smith 1990; Ge & Garven 1994; Eichhubl *et al.* 2004). A number of fluid sources and flow regimes are possible in orogens, including deep, diffuse flow of devola-

	G	F	L	1	4	6	B	Dispatch: 17.4.06	Journal: GFL	CE: Hari
	Journal Name			Manuscript No.				Author Received:	No. of pages: 14	PE: Meera Moydn

tilized metamorphic and magmatic fluids being driven by orogenic stresses (Oliver 1986) and shallow focused flow of meteoric fluids through foreland thrust sheets and foreland basins driven by topographic recharge (Ge & Garven 1994; Hutcheon *et al.* 2000). Orogenic aquifer systems may or may not be stratified with confined zones between which there is no mixing or exchange of fluids, but through which there is fluid flow and fluid–rock interaction (Fig. 1; Koons & Craw 1991; Evans & Battles 1999).

The Montana recess of the Sevier orogeny includes the foreland thrust sheets of the Idaho–Montana thrust belt exposed from west to east in the Lost River, Lemhi, and Beaverhead Ranges and the Tendoy Mountains, which are separated by intervening Tertiary–Recent extensional basins. For the Lost River Range, which exposes Late Paleozoic carbonates deformed at depths of 5–8 km or more within the orogenic wedge, Davidson *et al.* (1998), Bebout *et al.* (2001) and Anastasio *et al.* (2004) inferred deep penetration of meteoric fluids from the isotopic compositions of synorogenic veins and variably deformed tectonite samples. To the east, along the thrust front, the emergent Four Eyes Canyon and Tendoy thrust sheets emplaced Late Paleozoic carbonates and clastics into a terrestrial foreland basin (Perry & Sando 1983; Haley & Perry 1990; Harkins *et al.* 2004a,b). Cretaceous thrusting near the orogenic surface resulted in discontinuous mineralized fractures that preserve a record of the geometry, physical conditions, and chemical composition of synorogenic fluid flow. Extensive exposures within several regional thrust sheets, from the basal décollement to well-preserved overlying synorogenic deposits, make the Tendoy Mountains, Montana, ideal for evaluating spatial and temporal variability in fluid sources and fluid–rock interactions during orogeny.

In this paper, we characterize the sources and pathways of synorogenic fluids affecting the Sevier foreland during Late Cretaceous–Eocene, a time of shifting orogenic kinematics and paleogeography. Shallow subduction of the Farallon plate during the Cretaceous resulted in the emplacement of basement and cover thrust sheets in the

Montana foreland close to the western shores of the Western Interior Seaway (Burchfiel & Davis 1975). Subsequent foundering of the Farallon slab in the Tertiary resulted in a tectonic transition from NE–SW contraction to E–W extension coincident with and subsequent to the northward retreat of the seaway from the Sevier foreland basin. Stable isotope compositions of veins and faults fingerprint meteoric fluids, of varying sources, that infiltrated the orogenic wedge during the transformation of the synorogenic paleogeography from an environment proximal to an oceanic shoreline to one increasingly interior–continental. We apply structural and petrographic analyses, stable isotope geochemistry, and fluid inclusion microthermometry to understand the synorogenic evolution of fluid pathways and sources. Sampling sites were selected to allow examination of fluid flow within and across major thrust sheets near the Sevier thrust front, and to explore variations in fluid–rock interaction as a function of structural position and strain history within individual faults and folds.

GEOLOGY AND STRATIGRAPHY OF THE TENDOY MOUNTAINS

The Tendoy and Beaverhead Mountains contain the frontal thrust sheets of the Sevier fold and thrust belt in southwestern Montana (Fig. 2). The Tendoy Mountains have experienced two major periods of deformation, both of which resulted in the development of systematic, synkinematic veins. Volcanics, interbedded with syntectonic Beaverhead Group conglomerates further north in the Beaverhead Range, were used to establish the emplacement of the frontal Erdmont fault at 79–76 Ma (Kalakay *et al.* 2001; Kalakay 2001). Like the Erdmont thrust, the Tendoy thrust in southwest Montana is an easternmost emergent thrust sheet carrying Paleozoic carbonates over synorogenic foreland basin sediments. Late Cretaceous to Paleocene pollenomorphs were described from the Beaverhead Group in the Tendoy Mountains, establishing thrust emplacement during this time (Perry *et al.* 1988; Skipp 1988). In the Tendoy thrust sheet, fault-related fold axes are oriented perpendicular to the direction of fault emplacement, as interpreted from fault zone kinematic indicators (McDowell 1997). Impingement with the Laramide Blacktail–Snowcrest uplift induced out-of-sequence faulting of the Deadwood Gulch imbricate within the Tendoy thrust sheet (Perry *et al.* 1983, 1988; McDowell 1992, 1997), and likely reactivated the Four Eyes Canyon thrust in the Late Cretaceous (Anastasio *et al.* 2002). Eocene pyroclastics and scattered lava flows were coincident with extensional faulting (e.g., the Muddy Creek graben), in the Four Eyes Canyon thrust sheet (Janecke *et al.* 1999). The Tendoy thrust sheet does not record large-scale normal faulting (Fig. 2). Samples of calcite veins and limestone protoliths were collected from both contractional

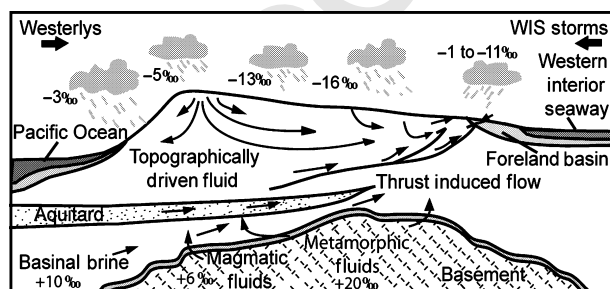
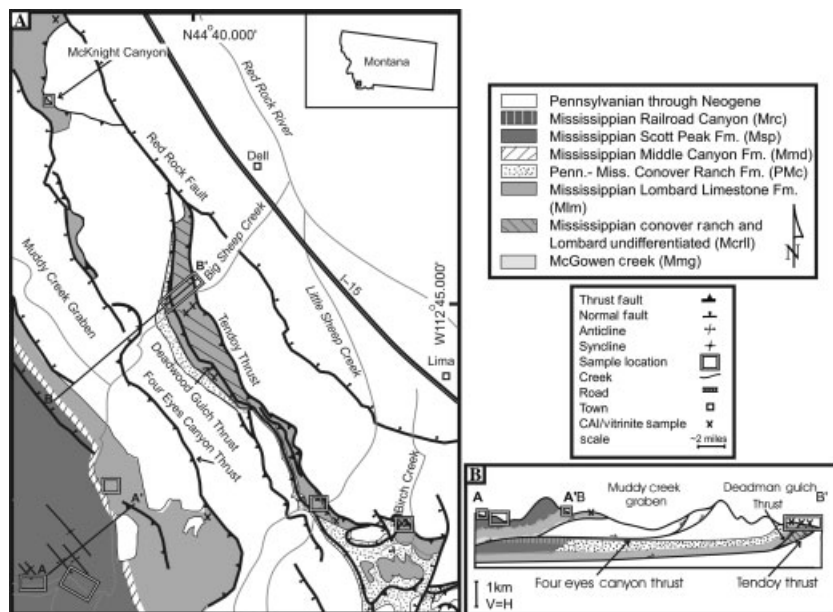


Fig. 1. Cartoon of fluid flow regimes in a fold and thrust belt setting: different fluid sources, $\delta^{18}\text{O}$ compositions, pathways, and driving mechanisms (modified from Koons & Craw 1991; Anastasio *et al.* 2004).

Fig. 2. (A) Simplified geologic map of the Sevier thrust front, Montana recess (after Lonon *et al.* 2000; Harkins 2002; Harkins *et al.* 2004a,b) showing position of sampling traverses for this study and color alteration index (CAI) and vitrinite reflectance data reported by Perry *et al.* (1983). (B) Cross section constructed through the Tendoy Mountains along Big Sheep Creek, with sample locations projected onto the cross section. The approximate structural and stratigraphic positions of CAI and vitrinite reflectance samples collected by Perry *et al.* (1983) are shown.



and extensional structures in a cross-sectional transect through the Four Eyes Canyon and Tendoy thrust sheets along Big Sheep Creek valley. To investigate strike-parallel variability within a thrust sheet, samples were collected from the basal Tendoy thrust zone at Birch Creek, Little Sheep Creek, Big Sheep Creek, and McKnight Canyon, an overall strike length in excess of 32 km (Fig. 2). Sampling focused on the Mississippian Lombard Limestone, which lies in the immediate hanging wall of the Tendoy fault, as well as from the Lombard Limestone and overlying Scott Peak Formation (also limestone) of the Four Eyes Canyon thrust sheet (Fig. 2). Sampling at Birch Creek focused on fault-related folds in the hanging wall of the Tendoy sheet, approximately 500 m up-section from an exposure of the fault. Sampling at the Little Sheep Creek, Big Sheep Creek, and McKnight Canyon localities focused on the immediate hanging wall of the main Tendoy thrust or a leading edge imbricate. Further west, along the Big Sheep Creek traverse, samples were collected at three locations in the folded hanging wall of the Four Eyes thrust sheet (Fig. 2).

VEIN GENESIS

Vein textures

More than 60 oriented samples representing the diversity of vein sets in the Tendoy and Four Eyes Canyon thrust sheets were collected. Twenty vein samples were studied petrographically to establish mineralization textures from which we reconstructed a history of fluid flow. Vein fillings are either sparry or fibrous and either comprise a single layer inferred to form from a single fluid charge or have multiple layers, recording multiple opening and mineraliza-

tion events (Fig. 3). The majority of the veins consist of euhedral crystals that range in size from 6 to 120 μm . Generally, vein fillings nucleate from wall-rock seed crystals on both sides of the fracture and expand in size toward the vein center (Fig. 4). Some vein layers contain fragments of wall-rock limestone. In some veins, protolith clasts served as nucleation sites for euhedral calcite rosettes with large crystals, 1–8 cm in length. The Tendoy thrust sheet contains both fibrous bedding-parallel veins and steep (relative to bedding) veins filled with a single generation of sparry calcite. In contrast, bedding-parallel, Scott Peak Formation veins in the western Four Eyes Canyon thrust sheet consist of coarse calcite spar or are multi-layered, crack-seal veins. These textures are indicative of hydraulic fracturing and subsequent vein mineralization within a water sill and require periodic fluid pressures in excess of lithostatic pressure (e.g. Henderson *et al.* 1990; Fisher & Brantley 1992; Cosgrove 2001). In some cases, textural and color variation between layers indicate up to 12 cycles of cracking and sealing. The Four Eyes Canyon thrust sheet also contains a set of high-angle veins transecting folds and some bed-parallel veins, which were active during Eocene extensional deformation. In the host rock carbonate, rare cleavage selvages reflect localized pressure solution strain.

Vein orientation and kinematics of vein development

Orientation analyses of bedding within the Tendoy thrust sheet are shown in Fig. 5A. A cylindrical best fit to the data indicates a mean fold axis for the Tendoy thrust sheet of $322^\circ/06^\circ$ (trend/plunge). The northwestern strike of the thrust sheet and numerous mesoscopic northeast ver-

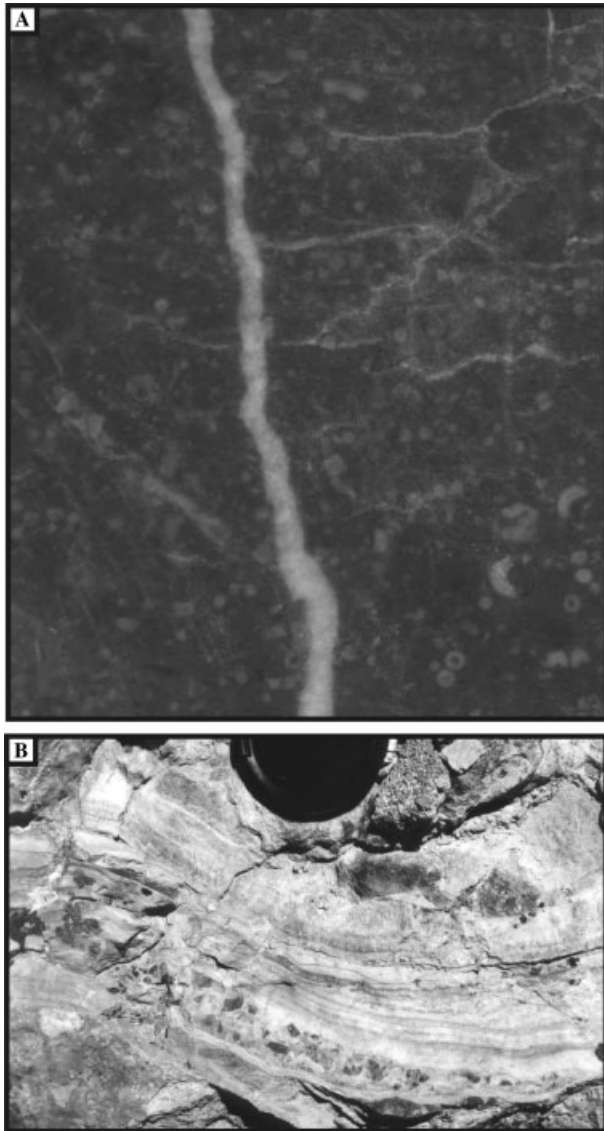


Fig. 3. (A) Example of a simple extensional vein, 3 mm wide, in cut specimen. (B) Example of a complex, multi-layered vein in field photograph – various layers represent different periods of vein mineralization and are identified by textural and color variation, camera lens cap about 6 cm.

ging asymmetric, horizontal folds are consistent with northeastward thrust emplacement. In the Four Eyes Canyon thrust sheet, structural trends are similar to those of the Tendoy thrust sheet with a composite fold axis oriented $330^{\circ}/13^{\circ}$ (Fig. 5B). Average fold axes were used to untilt bedding to evaluate the temporal evolution of fracturing and fluid flow recorded by veins during fault-related folding.

Several pervasive, systematic sets of calcite-filled veins occur throughout the frontal thrust sheets. Vein orientations were assessed in both geographic coordinates and in unfolded flat-lying beds, termed stratigraphic coordinates. Typically, brittle structures, such as joints, veins, and faults



Fig. 4. Multiple layered vein showing bi-directional growth of calcite off seed nuclei on the vein walls inward toward the center where crystals enlarge. A few of the larger calcite crystals exhibit mechanical twin lamellae.

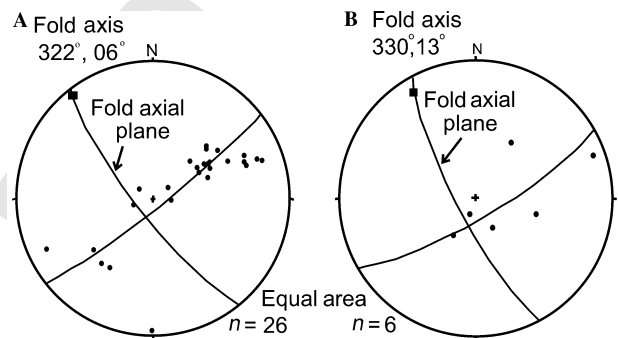


Fig. 5. (A) Lower hemisphere stereographic projection of poles to bedding in the Tendoy thrust sheet and (B) poles to bedding in the Four Eyes Canyon thrust sheet.

occur in sets with common orientations relative to regional-scale stress regimes and structures. Crosscutting relationships between various sets of disjunctive features provides evidence to establish strain history. We use consistency of orientation to evaluate the timing between faulting, folding and fracturing. This assumes that veins with common orientation share a common genesis (e.g., Dunne & Hancock 1994). The following sections separately analyze the orientation of veins in the Tendoy and Four Eyes Canyon thrust sheets.

Tendoy thrust sheet

Extensional (mode I) longitudinal veins striking parallel to fold axis and transverse veins oriented in the dip direction of beds, and bed-parallel shear (mode II) veins are present in the Tendoy thrust sheet (Fig. 5). These are common vein and joint orientations in foreland fold and thrust belts (Sterns 1969; Holl & Anastasio 1992; Tavernelli 1997). The longitudinal and transverse vein sets are pervasive with 0.5 m spacing (Fig. 6). Bed-parallel veins are restricted to

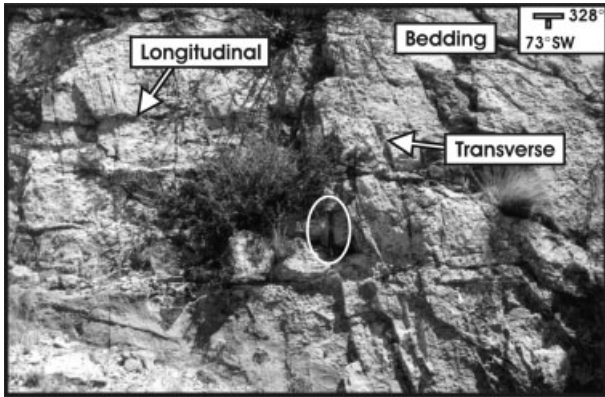


Fig. 6. Field photograph of a bedding plane exposure with systematic longitudinal (horizontal) and transverse (vertical) vein sets in the Mississippian Lombard Limestone at Little Sheep Creek (hammer for scale).

inclined bedding on fold limbs and are not found in flat-lying beds. Shear fibers and mineral accretion steps within some bedding-parallel veins record hingeward shear on fold limbs, consistent with flexural-slip fold kinematics. Excluding the narrow (approximately 1 m) brittle deformation zone of veined cataclasite in the immediate hanging/wall of the Tendoy thrust fault at the McKnight Canyon location, field observations reveal mutual cross-cutting relationships between the high-angle longitudinal and transverse veins, whereas, bed-parallel veins, cross-cut, and thus postdate, the high-angle vein sets. As younger bed-parallel veins were related to folding, older, longitudinal and transverse veins of the Tendoy thrust sheet were analyzed in stratigraphic coordinates (Fig. 7). In stratigraphic coordinates the two distinct populations of veins within the Tendoy thrust sheet have mean orientations of N057°E (strike), 85°NW (dip, dip direction) and N147°E, 87°SW (Fig. 7). These pre-folding veins represent a transverse vein set, parallel to regional shortening direction, and a longitudinal set parallel to the strike of the Tendoy thrust fault. A summary of the vein geometry and kinematics for the Tendoy thrust sheet during regional Cretaceous compression is provided in Fig. 7.

Four Eyes Canyon thrust sheet

In the Four Eyes Canyon thrust sheet three distinct vein set orientations are related to Cretaceous contraction; oriented 068°/84° SE, 159°/66° SW, and bed-parallel in geographic coordinates (Fig. 8). The strike of the transverse vein set is nearly parallel to the dip directions of bedding and the longitudinal set is oriented approximately parallel to the regional strike (Fig. 5). The longitudinal, transverse, and bed-parallel veins are all mutually cross-cutting in the Four Eyes Canyon thrust sheet (Fig. 8). Orientations of steep Four Eyes Canyon thrust sheet veins do not show improved dispersion in stratigraphic coordinates when compared with geographic coordinates and thus are

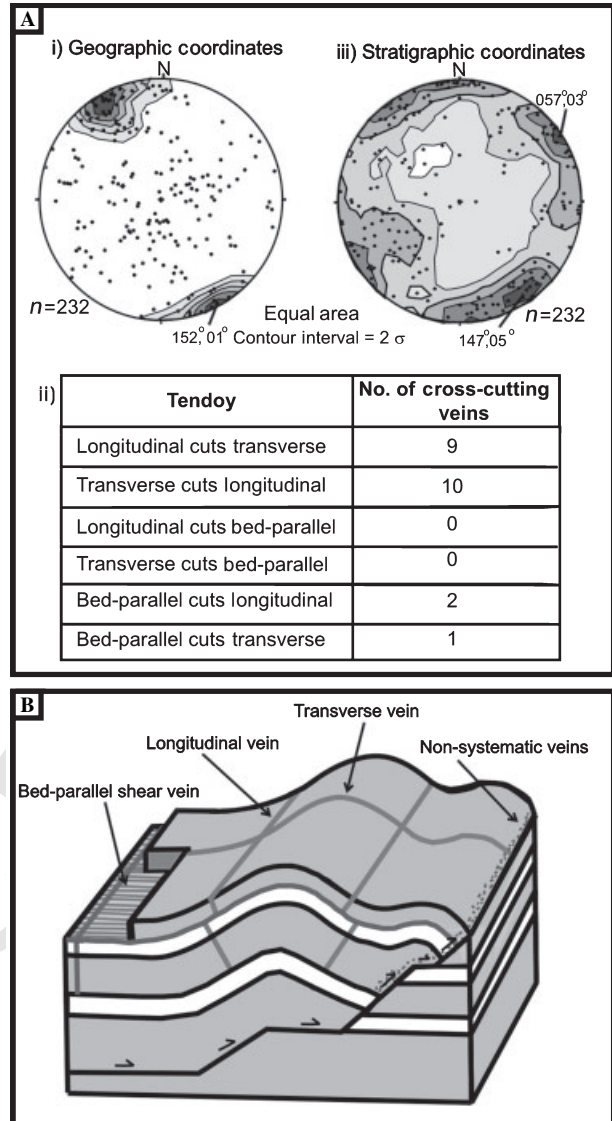


Fig. 7. (A) Orientation analysis of veins from the Tendoy thrust sheet. (i) Lower hemisphere stereographic projection of poles to all Tendoy veins in geographic coordinates, with dispersion shown by 2σ standard deviation. (ii) Table of observed cross-cutting relationships between different vein sets (represents 11% of veins). (iii) Lower hemisphere stereographic projection of poles to veins in stratigraphic coordinates, bedding horizontal. (B) Schematic illustration of Tendoy vein sets.

interpreted to have formed during, rather than before, folding and thrust sheet emplacement. Additional high-angle systematic, but irregular, veins cut decimeter-scale folds in the Four Eyes Canyon thrust sheet and reactivate portions of bed-parallel and longitudinal veins as they cut up through the stratigraphy. Because these extensional veins consistently transect contractional structures, they are interpreted to have formed subsequent to Cretaceous deformation. The irregular veins formed in proximity to regional-scale extensional structures known to be active

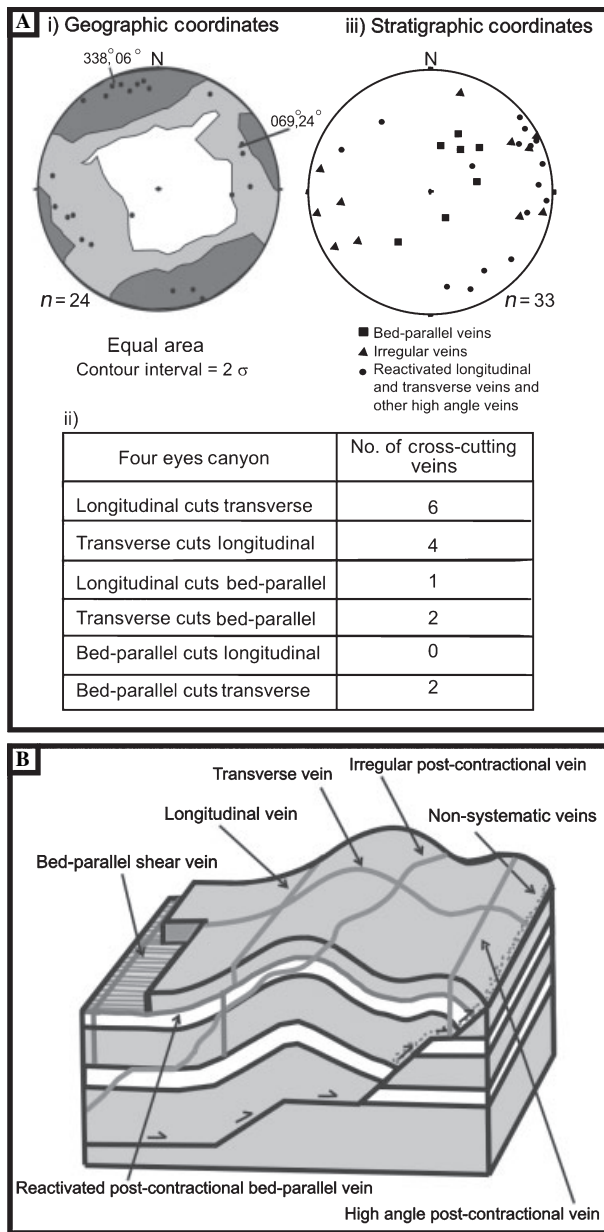


Fig. 8. (A) Orientation analysis of Four Eyes Canyon thrust sheet veins. (i) Lower hemisphere stereographic projection of poles to Cretaceous veins in geographic coordinates. (ii) Table of observed cross-cutting relationships between different vein sets (represents 8% of veins). (iii) Lower hemisphere stereographic projection of Eocene veins in stratigraphic coordinates. (B) Schematic illustration of Four Eyes Canyon vein sets.

during the Eocene (e.g. Muddy Creek graben; Janecke *et al.* 1999) and are therefore interpreted to record mineralization during Eocene extension. The Tendoy thrust sheet lacks both large-scale extensional faults and the late stage irregular extensional veins. A summary of the Four Eyes Canyon thrust sheet vein geometries and kinematics is provided in Fig. 8.

DISCUSSION

Deformation conditions

Knowledge of the environmental conditions during deformation is key in determining fluid compositions and sources as temperature has a large effect on the fractionation of oxygen isotopes between calcite and low-temperature aqueous fluids. Tendoy and Beaverhead Mountain carbonates contain sparse calcite grains with one or two sets of thin mechanical twin lamellae, indicative of temperatures $<200^{\circ}\text{C}$ (Ferrill 1991). Perry *et al.* (1981, 1983) reported conodont and vitrinite data from the Tendoy and Four Eyes Canyon (what they called the Medicine Lodge thrust) thrust sheets along the study corridor. This study of organic maturation helps constrain temperature conditions during deformation along the southwestern Montana thrust front. Conodont and vitrinite reflectance sample locations proximal to our sample sites are shown in Fig. 2. Conodont color alteration index (CAI) values of 1 from the Tendoy thrust sheet indicate peak temperatures $<50^{\circ}\text{--}80^{\circ}\text{C}$ (Epstein *et al.* 1977; Perry *et al.* 1981). Vitrinite reflectance values from Mississippian rocks of 0.35% R_o (Perry *et al.* 1981), indicate peak temperatures of 51°C based on calibration data of Barker & Pawlewicz (1994). Perry *et al.* (1983) inferred a paleo-geothermal gradient of $20^{\circ}\text{C km}^{-1}$, equivalent to the modern gradient from a deep drill-hole within the nearby Centennial Basin. However, the modern gradient is certainly influenced by extensive Tertiary to Holocene extension and volcanism, including nearby passage of the Yellowstone hotspot. Wedge-top and foreland basins developed on old crust typically have cooler geothermal gradients. The Tendoy thrust sheet was at least 2300 m thick to accommodate the translated preorogenic Mississippian-Cretaceous section and with the likely addition of several hundred meters of now eroded Cretaceous syntectonic conglomerates a maximum burial depth of approximately 3 km was postulated by Perry *et al.* (1983) for the thrust sheet. Using a mean surface temperature of 20°C , and a geothermal gradient of $15^{\circ}\text{C km}^{-1}$ (e.g., Holl & Anastasio 1995 for the Pyrenean wedge-top basin) yields a maximum temperature estimate of 65°C for the base of the Tendoy thrust sheet, consistent with organic maturation values, which develop as a function of both time and temperature. In the Four Eyes Canyon thrust sheet conodont color alteration values are approximately 1.5 and are interpreted by Perry *et al.* (1983) to record burial depths of approximately 4 km and hence a peak thrust temperature of 80°C .

Vein textures in bedding-parallel veins in the western Four Eyes Canyon thrust sheet are indicative of at least transient fluid pressures in excess of lithostatic pressure. At the western two Big Sheep Creek sample localities, we

identified extensive bedding-parallel veins with euhedral calcite within the lower Scott Peak Formation. This stratigraphic interval is confined between argillaceous limestone units. In the active carbonate thrust sheets of the western Taiwan thrust belt foreland, overpressure conditions are extensively developed between 3 and 5 km, but never shallower than 2 km (Suppe & Wittke 1977). Therefore, by analogy, we chose 2 km as the minimum depth for vein formation along the Sevier thrust front. This minimum depth and a geothermal gradient of $15^{\circ}\text{C km}^{-1}$ constrained the minimum temperature of 50°C and organic maturation values constrained our choice of 80°C for the maximum temperature during vein mineralization which we used when interpreting the stable isotope data for Cretaceous veins in the Four Eyes Canyon thrust sheet. Using similar logic, we chose a peak temperature range of $50\text{--}65^{\circ}\text{C}$ for the Cretaceous vein formation in the Tendoy thrust sheet.

Irregular Four Eyes Canyon veins were precipitated after Cretaceous compression, likely during the Eocene. The paleotemperatures during Eocene deformation are not as well constrained. These veins likely formed at depths shallower than those for the Cretaceous veins given the prior emergence of the thrust wedge and its subsequent exhumation. Extension and volcanism, which began during the Eocene, persists today so we adopt the modern geothermal gradient of $20^{\circ}\text{C km}^{-1}$ to estimate Eocene paleotemperatures. Cross-section reconstructions (Harkins 2002) suggest that the sampled veins developed at 2–3 km depth. Thus, we use temperatures of $60\text{--}80^{\circ}\text{C}$ when interpreting isotopic data for the Eocene veins.

Fluid inclusion analysis

Fluid inclusion microthermometry of vein minerals were attempted on 13 representative samples in order to obtain fluid homogenization temperatures and composition constraints on the mineralizing fluids. In general, inclusions were small, 2–5 μm , secondary, and located along healed microfractures. Many inclusions were decrepitated so were not useful in finding the homogenization temperature. Phase changes were induced in vapor bubbles in two inclusions from Cretaceous-age Tendoy thrust sheet veins. These provided homogenization temperatures of $+44$ and $+160^{\circ}\text{C}$. The large difference between these homogenization temperatures led us to rely on the organic maturation results and burial reconstructions to estimate temperatures of vein precipitation. In the absence of direct data on fluid temperatures, we use the reasonable assumption that rock and fluid temperatures were similar during vein mineralization.

Fluid density and salinity were determined from inclusion melting temperatures (e.g., Roedder 1984). Increased salinity depresses the freezing point of aqueous fluids and those that retain their solid phase at temperatures above

0°C indicate very low-salinity water (Roedder 1984). Melting temperatures obtained from the Tendoy samples of -0.6 and $+3.6^{\circ}\text{C}$ indicate freshwater fluid inclusions. Other inclusions along the same healed microfractures were stained brown with bitumen residue indicating simultaneous migration of freshwater and hydrocarbons (cf., Burruss 1981). An exploration well at McKnight Canyon, in the immediate Tendoy footwall, recorded hydrocarbon shows (Amoco Production Company 1986) and Swetland *et al.* (1978) identified petroleum source rocks in black shales, found interbedded in the basal Mississippian carbonates of the Tendoy thrust sheet.

Fluid compositions and sources

Stable isotope analyses

Stable isotope analyses were conducted on wall rocks, veins, microlithons, and cleavage selvages within the Tendoy and Four Eyes Canyon thrust sheets. Microsamples of vein calcite and carbonate protoliths were processed for oxygen and carbon stable isotope analyses following conventional techniques (McCrea 1950), and the liberated CO_2 gas was analyzed in dual-inlet mode on the Finnigan MAT 252 spectrometer at Lehigh University. Oxygen and carbon isotopic values are reported relative to Vienna standard mean ocean water (V-SMOW) and PeeDee Belemnite (PDB), respectively, and reported in conventional delta (δ) notation, in per mil (‰):

$$\delta^{18}\text{O} = 1000\left[\left(\frac{^{18}\text{O}/^{16}\text{O}}{^{18}\text{O}/^{16}\text{O}}\right)_{\text{sample}} / \left(\frac{^{18}\text{O}/^{16}\text{O}}{^{18}\text{O}/^{16}\text{O}}\right)_{\text{standard}} - 1\right] \quad (1)$$

$$\delta^{13}\text{C} = 1000\left[\left(\frac{^{13}\text{C}/^{12}\text{C}}{^{13}\text{C}/^{12}\text{C}}\right)_{\text{sample}} / \left(\frac{^{13}\text{C}/^{12}\text{C}}{^{13}\text{C}/^{12}\text{C}}\right)_{\text{standard}} - 1\right] \quad (2)$$

Standardization of isotopic results was verified using well-characterized internal laboratory (calcite 8-3-7v- CO_3) and international carbonate standards, indicating uncertainties (expressed as 1σ) of 0.15‰ and 0.1‰ for $\delta^{18}\text{O}$ and $\delta^{13}\text{C}$, respectively.

Large variation was observed in both $\delta^{18}\text{O}$ and $\delta^{13}\text{C}$ in microsampled vein calcite. Undeformed protoliths, vein host rocks, cleavage selvages and intervening microlithons in locally penetratively deformed samples have $\delta^{18}\text{O}$ values of $+20$ to $+27\text{‰}$ and $\delta^{13}\text{C}$ values of $+0.6$ to $+5.6\text{‰}$ (Fig. 9). Vein $\delta^{18}\text{O}$ is lower than that of adjacent wall rock with only a few exceptions (Fig. 9). Cretaceous Tendoy thrust sheet veins show a range of $\delta^{13}\text{C}$ values from -0.9 to $+4.8\text{‰}$ and a range of $\delta^{18}\text{O}$ from $+8.9$ to $+28.8\text{‰}$ (Fig. 10). The more ^{18}O -enriched veins have $\delta^{18}\text{O}$ similar to that of the undeformed protoliths and vein wall rocks. Bed-parallel fibrous veins have higher $\delta^{18}\text{O}$ values, in the range of undeformed protolith, whereas thrust zone cataclastic veins (fault breccia) have somewhat lower $\delta^{18}\text{O}$ values

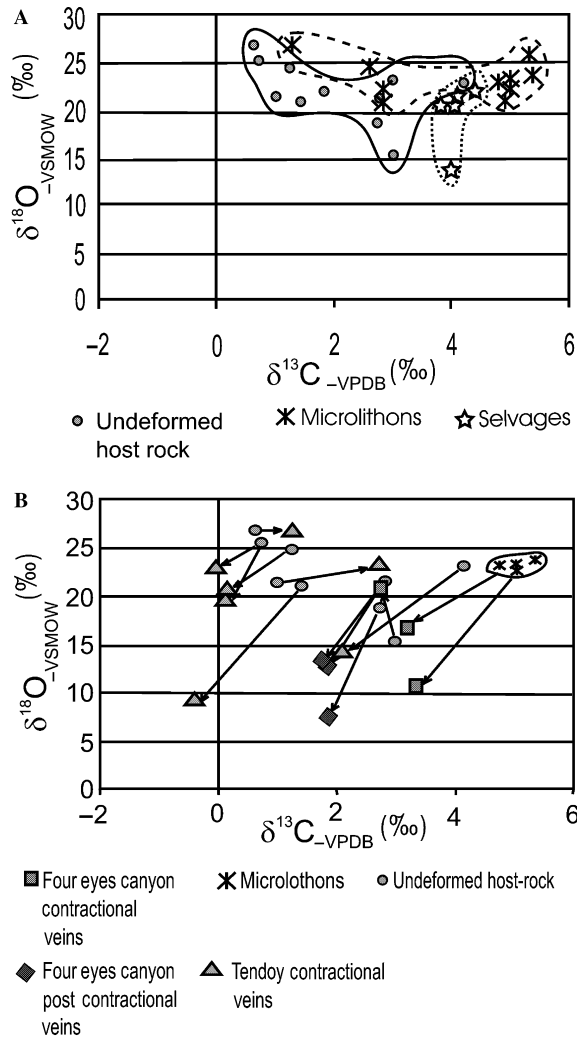


Fig. 9. (A) Undeformed host-rock, microlithons, and selvages in deformed samples have $\delta^{18}\text{O}$ compositions with a mean of $+22.2\text{‰}$ and a standard deviation of $\pm 3\text{‰}$. This range is shown on other plots as a shaded region. (B) Tie lines between host-rock and corresponding vein analysis.

(Fig. 10A). One Tendoy thrust sheet longitudinal vein varies by 15‰ in $\delta^{18}\text{O}$ (Fig. 10B), showing nearly the same range in $\delta^{18}\text{O}$ as all other samples from this thrust sheet (compare with Fig. 10A), seemingly indicating evolving $\delta^{18}\text{O}$ of the vein-forming fluids. In this vein, the lower- $\delta^{18}\text{O}$ regions have $\delta^{13}\text{C}$ ($+0.22$ and $+1.0\text{‰}$) lower than that of the higher- $\delta^{18}\text{O}$ regions ($\delta^{13}\text{C} = +2.5$ to $+5.0\text{‰}$).

In the Four Eyes Canyon thrust sheet, veins thought to be Cretaceous in age (Sevier orogenic contraction) have $\delta^{18}\text{O}$ values of $+5.2$ to $+20.9\text{‰}$ (Fig. 11). Overall, the Sevier-age veins in the Four Eyes Canyon thrust sheet show slightly lower $\delta^{18}\text{O}$ and a smaller range in $\delta^{13}\text{C}$ when compared with the Tendoy veins (cf., Fig. 10). There is a longitudinal vein that has a $\delta^{18}\text{O}$ value of $+13\text{‰}$, lower than that of the wall rock and within the range of other Four Eyes Canyon and Tendoy Sevier-age veins (Fig. 11).

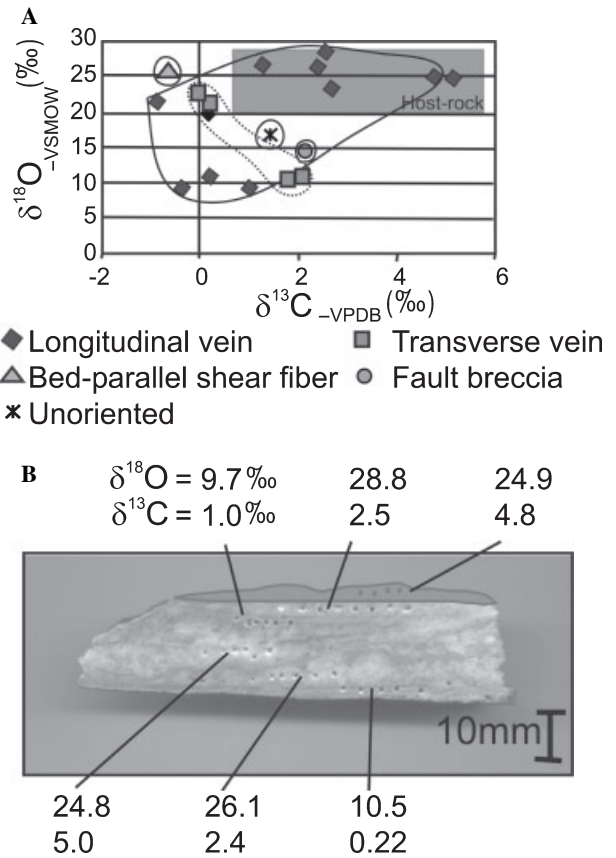


Fig. 10. Cretaceous Tendoy thrust sheet veins. (A) Plot of all Tendoy thrust sheet isotope data. (B) Multigenerational vein sample from the Tendoy thrust sheet. Spots are microsample locations for stable isotope analyses of vein material.

One Four Eyes Canyon bed-parallel vein has a $\delta^{18}\text{O}$ value considerably lower than that of a bed-parallel vein from the Tendoy thrust sheet (cf., Figs 10A and 11A). A penetratively deformed Cretaceous Four Eyes Canyon hand sample was analyzed in more detail to identify any variations in isotopic composition among microlithons, cleavage selvages, and vein calcite (Fig. 11B). For this sample, mean $\delta^{18}\text{O}$ of cleavage selvages ($\delta^{18}\text{O} = +21.6$, $1\sigma = 0.70$; $n = 4$) is somewhat lower than mean $\delta^{18}\text{O}$ of the microlithons in the same sample (for microlithons, mean $\delta^{18}\text{O} = +23.2$, $1\sigma = 0.50$; $n = 4$), and lower than the overall $\delta^{18}\text{O}$ range for protoliths documented for undeformed host-rocks across the region (Fig. 9). Veins in this sample have even lower $\delta^{18}\text{O}$ values (two veins with mean $\delta^{18}\text{O}$ of $+10.6$ and $+17\text{‰}$).

Four Eyes Canyon veins believed to have developed in the Eocene during regional extension, have $\delta^{18}\text{O}$ values of $+5.9$ to $+21.6\text{‰}$, but mostly have $\delta^{18}\text{O}$ lower than $+15\text{‰}$ (Fig. 12). One Eocene-age, multi-layered vein from the Four Eyes Canyon thrust sheet has relatively uniform $\delta^{18}\text{O}$ in sequentially mineralized fracture fillings, independent of position in the vein (Fig. 12B; for five analyses, mean

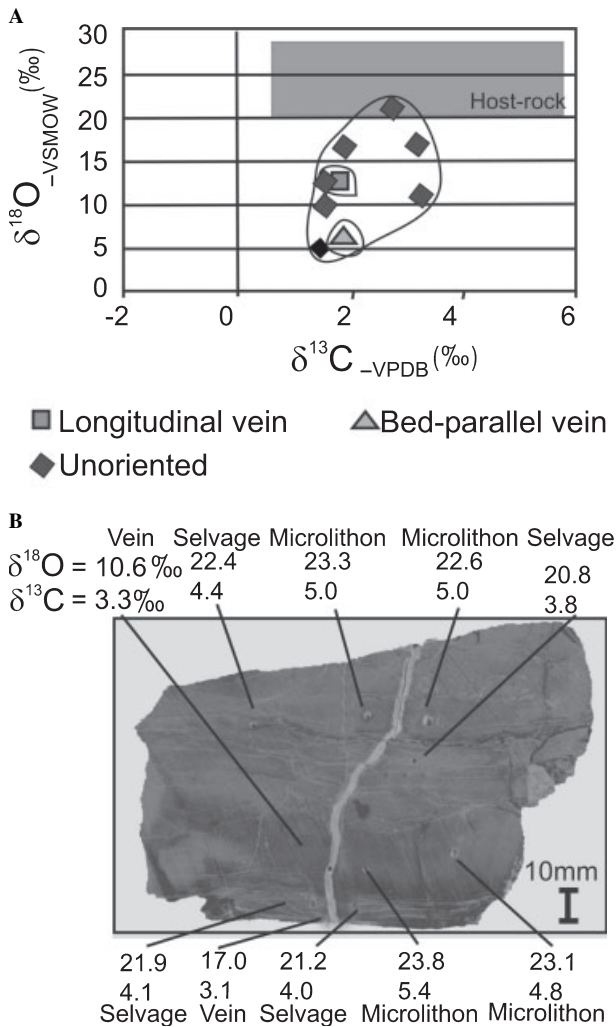


Fig. 11. Cretaceous Four Eyes Canyon veins. (A) Cretaceous Four Eyes Canyon isotopic data. (B) Sample from the Four Eyes Canyon thrust sheet, microlithons, selvages, and vein analysis. Note that microlithon and selvage data for the sample shown in B are not plotted in A.

$\delta^{18}\text{O} = +12.7$, $1\sigma = 0.04$). The systematic difference between undeformed host rocks with high $\delta^{18}\text{O}$ to lower $\delta^{18}\text{O}$ in Four Eyes Canyon thrust sheet veins is a pattern seen throughout the thrust front (cf., Figs 9–11). Another Eocene vein sampled from the Four Eyes Canyon thrust sheet shows a larger range in $\delta^{18}\text{O}$ (overall range of +5.9 to +12.5‰), with a suggestion of two distinct compositions with mean $\delta^{18}\text{O}$ near +12.4 and +6.6‰ (Fig. 12C). For both Four Eyes Canyon veins sampled in more detail (Fig. 12B,C), vein $\delta^{13}\text{C}$ (+1.2 to +2.2‰) is lower than that of host-rocks (+2.8 to +3.0‰).

Interpretation of isotopic results

The existence of bed-parallel shear veins in the Tendoy thrust sheet with $\delta^{18}\text{O}$ values similar to the undeformed host-rock is consistent with shear fiber growth by local

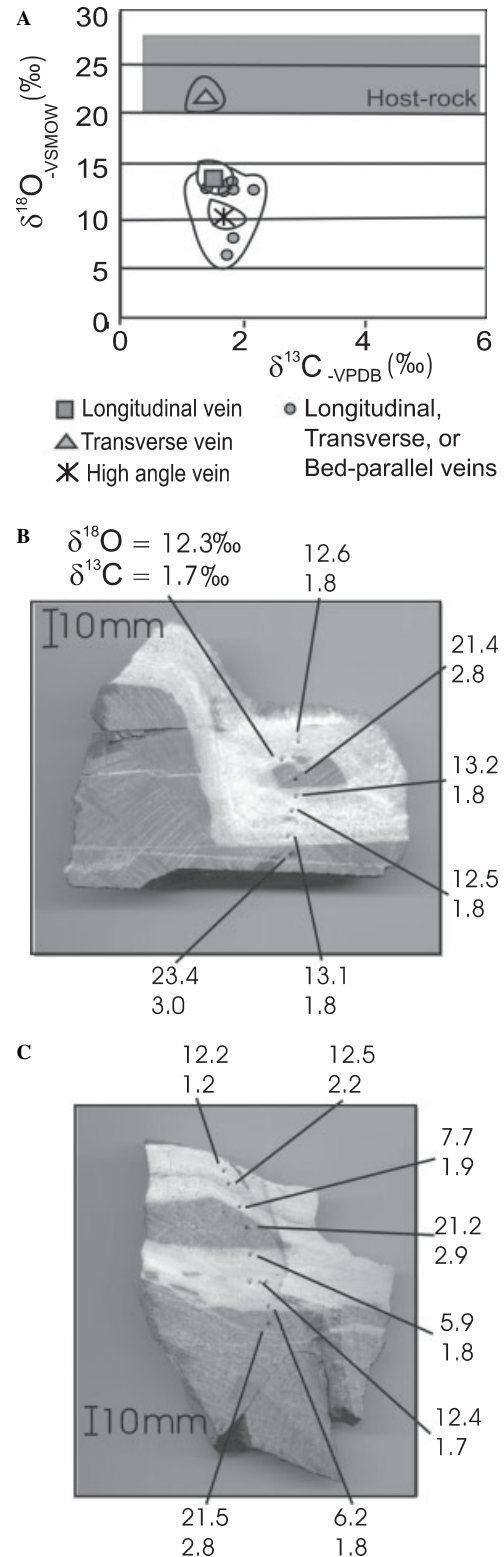


Fig. 12. Eocene Four Eyes Canyon veins. (A) Eocene vein isotopic data from the Four Eyes Canyon thrust sheet. (B) Multigenerational vein sample from the Four Eyes Canyon thrust sheet, data is included in plot. (C) Multi-generational, longitudinal vein sample from the Four Eyes Canyon thrust sheet, data is included in plot A.

diffusion (Durney 1972) and bed-scale closed system behavior. For high-angle veins in both thrust sheets and sparry bed-parallel veins in the Four Eyes Canyon thrust sheet, there are systematic shifts from higher- $\delta^{18}\text{O}$ host-rocks to lower- $\delta^{18}\text{O}$ veins. This implies that the fluids were not previously equilibrated with the host rock and instead were replenished from an external reservoir out of O-isotopic equilibrium with vein wall rocks. The variation in $\delta^{13}\text{C}$ is likely related to both stratigraphic differences between carbonate units (e.g., Anastasio *et al.* 2004) and varying exchange with migrating hydrocarbons. Fluid $\delta^{18}\text{O}$ (as H_2O) was calculated using vein $\delta^{18}\text{O}$ values and published calcite- H_2O fractionation factors for O isotope equilibrium (O'Neil *et al.* 1969). For the Sevier-age fluids, using temperature ranges of 50–80°C for the Four Eyes Canyon veins and 50–65°C for the Tendoy veins, calculated $\delta^{18}\text{O}$ values for H_2O in equilibrium with the vein calcite are as low as -18.5‰ for the Four Eyes Canyon veins (based on the use of $+5.2\text{‰}$ as a minimum value; overall calculated range for $\text{H}_2\text{O} = -18.5$ to -14.2‰) and are as low as -14.8‰ for the Tendoy thrust sheet veins (based on the use of $+8.9\text{‰}$ as a minimum value; overall calculated range for $\text{H}_2\text{O} = -14.8$ to -12.5‰). Calculated H_2O $\delta^{18}\text{O}$ values for the veins produced in the Eocene (-16.3 to -13.5‰) are similar to values for the Cretaceous-age veins, which show an overall range of -18.5 to -12.5‰ . In general, undeformed host rock, microlithons, and selvages have high $\delta^{18}\text{O}$ values ($+20$ to $+27\text{‰}$), which are consistent with values for marine carbonate rocks (Bebout *et al.* 2001).

With varying degrees of fluid–rock interactions involving high- $\delta^{18}\text{O}$ lithologies, a range of fluid compositions between the $\delta^{18}\text{O}$ of host rocks and extra-basinal fluids is expected (Rye & Bradbury 1988; Nesbitt & Muehlenbachs 1989, 1991; Davidson *et al.* 1998; Bebout *et al.* 2001; Anastasio *et al.* 2004). Fluids from deeper crustal sources, such as magmatic fluids ($\delta^{18}\text{O}$ values of $+5$ to $+10\text{‰}$, Sheppard 1996) and metamorphic fluids ($\delta^{18}\text{O}$ values up to $+20\text{‰}$, Nesbitt & Muehlenbachs 1989, 1991; Evans & Battles 1999), interacting with protolith carbonates are incapable of producing the observed low vein $\delta^{18}\text{O}$. Whereas, meteoric fluids, which typically have isotopic values less than 0‰ (Kendall *et al.* 1995) provide a fluid isotopic reservoir capable of generating the low $\delta^{18}\text{O}$ values in vein minerals of the Tendoy and Four Eyes Canyon thrust sheets. Low- $\delta^{18}\text{O}$ cataclastic veins along the Tendoy thrust fault records meteoric infiltration to at least the base of the thrust sheet. The lowest- $\delta^{18}\text{O}$ veins observed in each sample suite studied here could reflect less ‘upstream’ fluid–rock interaction in the thrust sheets (e.g., Rye & Bradbury 1988). Ocean water has a well-defined oxygen isotopic value of 0‰ and near-shore precipitation typically has an average $\delta^{18}\text{O}$ value of -5‰ (Kendall *et al.* 1995). Tropical storms, hurricanes (Lawrence & Gedzelman

1996), and steep topography can lead to the generation of precipitation with $\delta^{18}\text{O}$ values as low as -10‰ even near a coastline. As a result of inland evaporation and precipitation, rainfall in the modern Rocky Mountains (including along the study corridor) has $\delta^{18}\text{O}$ values as low as -22‰ and as high as -6‰ , including seasonal variation (Siegenthaler 1979; Yurtsever & Gat 1981; IAEA 2001; Peng *et al.* 2004). In the Late Cretaceous, during Tendoy thrust emplacement, the Western Interior Seaway coastline was positioned <100 km to the east of the thrust front and the western coast of North America was further inland than present (Fig. 13A). Western Interior Seaway $\delta^{18}\text{O}$ values

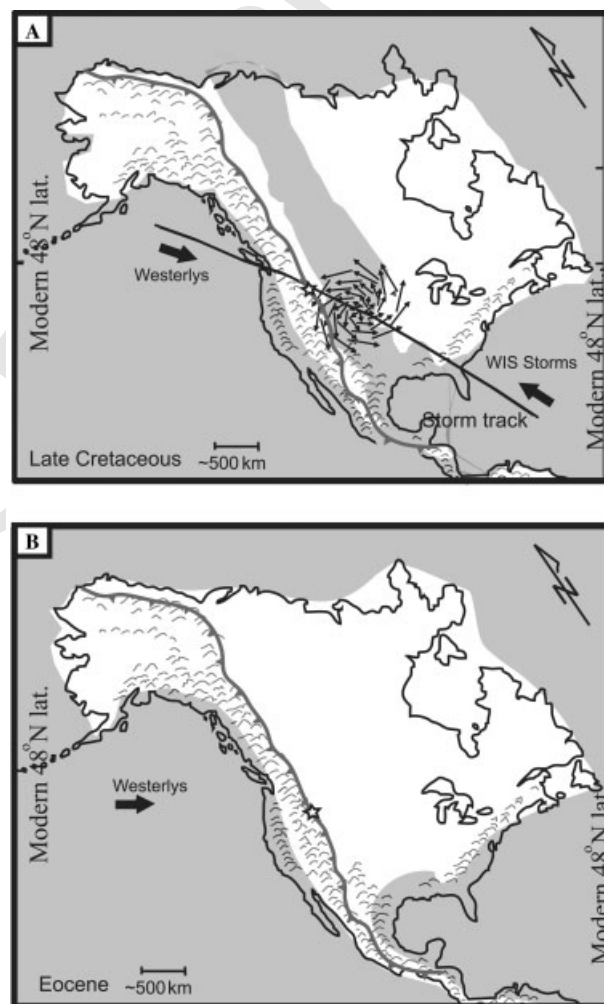


Fig. 13. (A) Paleogeographic map and the location of the Western Interior Seaway during the Late Cretaceous (Ericksen & Slingerland 1990). The frontal thrust of the Cordilleran Mountain Belt is shown and the study area is marked with a star in SW Montana. Modern North American shoreline is shown as reference. Climate models have determined that large cyclones blew across the seaway during the Cretaceous (e.g., Kump & Slingerland 1999). (B) Paleogeographic map of the Eocene (Scotese 2002), showing the location of the Pacific Ocean further to the west and the significant retreat of the Western Interior Seaway. The modern North American shoreline is shown for reference.

of -1‰ were inferred from calcareous, phosphatic, and siliceous skeletal material (Whittaker *et al.* 1987; Cadrin 1992; Cadrin *et al.* 1995). Paleoclimate reconstructions show that northern hemisphere circulation and storm tracks were from northwest to southeast across the seaway (Fig. 13) (e.g., Ericksen & Slingerland 1990; Jewell 1996; Sageman 1996; Slingerland *et al.* 1996; Kump & Slingerland 1999) and that a wet climate existed along the Montana thrust front (e.g., Jewell 1996).

The calculated minimum $\delta^{18}\text{O}$ values for the water in equilibrium with Cretaceous and Eocene veins in the study area are similar to values for aqueous fluids that infiltrated the Wildhorse Detachment Fault of the Eocene Pioneer core complex ($\delta^{18}\text{O}$ values of -14.7 to -17.7‰ , Bebout *et al.* 2001) and hydrothermal fluids, which interacted with Mississippian outer shelf carbonates at depths of 5–7 km and 150–400°C around the Eocene Idaho batholith ($\delta^{18}\text{O}$ values of -16‰ , Criss & Taylor 1983). These low- $\delta^{18}\text{O}$ isotopic signatures were interpreted as resulting from meteoric fluid–rock interaction. By the Eocene, the Western Interior Seaway had retreated (Fig. 13) and the surface hydrogeologic regime along the Rocky Mountain front was interior continental, similar to today. Although all of the calculated H_2O $\delta^{18}\text{O}$ values presented here are convincingly negative and point to a strong isotopic influence of meteoric waters, the relatively large uncertainties in the temperatures of vein formation produce large overlapping $\delta^{18}\text{O}$ ranges that prevent any assessment of temporal (Cretaceous to Eocene) evolution in meteoric water $\delta^{18}\text{O}$. Interestingly, further west in the Lost River Range, Idaho, higher calculated H_2O $\delta^{18}\text{O}$ values of -7.5 to $+2.5\text{‰}$, for temperatures of 150–250°C were interpreted as reflecting infiltration, in the Cretaceous, by meteoric fluids, influenced by proximity to the Western Interior Seaway (Davidson *et al.* 1998; Bebout *et al.* 2001; Anastasio *et al.* 2004). Differences in the calculated $\delta^{18}\text{O}$ values for infiltrating Cretaceous meteoric fluids across the Montana recess of the Sevier thrust belt might reflect deformation temperature uncertainties, synorogenic fluid compositional variations caused by topographic effects, proximity to the Interior Seaway or Pacific Ocean, or variation in precipitation isotopic composition (see Peng *et al.* 2004).

Studies by Davidson *et al.* (1998), Bebout *et al.* (2001), and Anastasio *et al.* (2004) further west within the Montana recess showed that veins formed during Sevier deformation could vary in isotopic composition based on the amount of upstream fluid–rock interaction ($\delta^{18}\text{O}$ $+5$ to $+27\text{‰}$). Some veins had $\delta^{18}\text{O}$ compositions that were similar to their meteoric fluid source, while others had compositions much closer to the surrounding carbonate protolith. The lower values, near -7.5‰ (Bebout *et al.* 2001), which are more similar to, but still somewhat higher than those calculated for Cretaceous veins in southwest Montana (-18.5 to -12.5‰ for calculated H_2O),

could better reflect the surface waters affecting that part of the thrust belt now exposed in the Lost River Range. Several other studies have shown a wide range of isotopic compositions in vein material along flow pathways. Oliver & Wall (1987) in Proterozoic calcilicates in the Mary Kathleen thrust belt of Queensland, Australia reported alteration of $\delta^{18}\text{O}$ of calcite from $+18.2$ to $+20.8\text{‰}$ to $+8$ to $+15\text{‰}$ resulting from infiltration by external fluids.

Isotopic results suggest that meteoric fluids infiltrated into the Sevier thrust sheets to the basal décollement along the thrust front to depths of at least 4 km in southwest Montana and 7–10 km in the Lost River Range, Idaho (Bebout *et al.* 2001; Anastasio *et al.* 2004). Studies in the Canadian Rocky Mountain foreland basin likewise show the infiltration of meteoric fluids to depths of 3–4 km along the thrust front (Nesbitt & Muehlenbachs 1991; Hutcheon *et al.* 2000) and to depths of 8 km in the Lewis thrust sheet of the Main Ranges (Price 2001). Modeling studies suggest topographic recharge in mountainous areas can drive meteoric fluids to significant depths (Koons & Craw 1991; Ge & Garven 1994) from which they ascend, driven by buoyancy forces, up-dip toward the foreland, mineralizing fractures along the way (Koons & Craw 1991). At least locally, topographic recharge in the low elevation, discharge end of the Sevier recess flow system generated periodic hydraulic fracturing. Vein textures indicative of overpressures and mineralization within water sills are restricted structurally to the Four Eyes Canyon thrust sheet and are isolated stratigraphically in the lower Scott Peak Formation, which is confined between lower permeability argillaceous limestones (e.g., Belitz & Bredenhoeft 1988).

The recognition of synorogenic meteoric fluid–rock interaction throughout the northern Rocky Mountains contrasts with the documentation of warm brines expelled as pore fluids and devolatilized as metamorphic fluids within the Appalachian fold and thrust belt (Evans & Battles 1999; Evans & Hobbs 2003). Eichhubl *et al.* (2004) identified basal fluid infiltration during Sevier contraction and the subsequent infiltration of meteoric fluids during Tertiary extension in the Great Basin, Nevada. Unfortunately, the relative uncertainty in temperature estimates for Cretaceous and Eocene vein formation along the Montana thrust front prevents an assessment of temporal evolution in meteoric water $\delta^{18}\text{O}$ that could be related to the retreat of the Western Interior Seaway.

CONCLUSIONS

This study demonstrates that the topographic recharge of meteoric waters can be fingerprinted and traced through an orogen. Fluid inclusion analysis of vein minerals, calculated burial reconstructions, and previously documented organic maturation values indicate low temperatures (up to

80°C) and shallow deformation (<4 km) for the emergent thrust sheets along Sevier deformation front in southwestern Montana. The $\delta^{18}\text{O}$ values of calcite veins from the Four Eyes Canyon and Tendoy thrust sheets are consistent with syntectonic infiltration by meteoric water with $\delta^{18}\text{O}$ of -18.5 to -12.5% . Structural analysis suggests Four Eyes thrust sheet veins were coincident with periodic overpressuring during thrust emplacement. Longitudinal veins in the Tendoy thrust sheet formed in flat lying rocks coincident with Four Eyes Canyon thrust sheet emplacement, whereas other Tendoy veins formed later, during Tendoy thrust sheet emplacement and folding. In the Eocene, some veins were reactivated and new veins were formed in the Four Eyes Canyon thrust sheet during regional extension. Eocene vein calcite also preserves O-isotopic signatures consistent with the infiltration of the orogen by meteoric waters (calculated H_2O $\delta^{18}\text{O} = -16.3$ to -13.5%). This study demonstrates the utility of stable isotopic data in assessing the interplay between surface hydrogeology and tectonic forcing.

ACKNOWLEDGEMENTS

The Geological Society of America and the American Association of Petroleum Geologists provided student research grants to Rygel. Mark Evans provided advice and the use of his fluid inclusion laboratory at the University of Pittsburgh. Lisa Chizmadia contributed unpublished data from a Lehigh undergraduate research project. Robert L. Johnson is thanked for field assistance and Nathan Harkins for his insights into the geology of the field area. We acknowledge thoughtful reviews by Peter Eichhubl and Andrew McCaig for *Geofluids*, and Grant Garvin is thanked for editorial advice. The research was conducted by Rygel in partial fulfillment of M.S. degree requirements at Lehigh University (under the name Adrienne C. Johnson).

REFERENCES

- Amoco Production Company (1986) *McKnight Canyon No.1, SE SW Section 21-T12S-R10W, Beaverhead County, Montana*. Amoco Production Company, Denver.
- Anastasio DJ, Harkins NW, Latta DK (2002) Coeval, in-and-out-of-sequence deformation within the frontal thrust sheets of the Tendoy Mountains, SW Montana. *Geological Society of America Rocky Mountain Sectional Meeting Abstract with Programs*, vol. 34, A7.
- Anastasio DJ, Bebout GE, Holl JE (2004) Extra-basinal fluid infiltration, mass transfer, and volume strain during folding: insights from the Idaho-Montana thrust belt. *American Journal of Science*, **305**, 333–69.
- Barker CE, Pawlewicz MJ (1994) Calculation of vitrinite reflectance from thermal histories and peak temperatures, a comparison of methods. In: *Vitrinite Reflectance as a Maturity Parameter, Applications and Limitations* (eds Mukhopadhyay PK, Dow WG), pp. ???–???. American Chemical Society, Washington, D.C.
- Bebout GE, Anastasio DJ, Holl JE (2001) Synorogenic crustal fluid infiltration in the Idaho-Montana thrust belt. *Geophysical Research Letters*, **28**, 429–4298.
- Belitz KR, Bredenhoeft JD (1988) Hydrodynamics of Denver Basin; explanation of subnormal fluid pressures. *American Association of Petroleum Geologists Bulletin*, **72**, 1334–59.
- Burchfiel C, Davis G (1975) Nature and controls of cordilleran orogenesis, western United States; extensions of an earlier synthesis. Tectonics and mountain ranges. *American Journal of Science*, **275-A**, 363–96.
- Burruss RC (1981) Hydrocarbon fluid inclusions in studies of sedimentary diagenesis. In: *Short Course in Fluid Inclusions. Applications to Petrology* (eds Hollister LS, Crawford ML), pp. 138–56. ?????.
- Cadrin AAJ (1992) Geochemistry and paleoenvironmental reconstruction of the Greenhorn marine cyclothem in the Western Interior Basin of Canada. PhD Thesis, University of Saskatchewan, Saskatchewan.
- Cadrin AAJ, Kyser TK, Caldwell WG, Longstaffe FJ (1995) Isotopic and chemical compositions of bentonites as paleoenvironmental indicators of the Cretaceous Western Interior Seaway. *Palaeogeography and Palaeoecology*, **119**, 301–20.
- Cosgrove JW (2001) Hydraulic fracturing during the formation and deformation of a basin: a factor in the dewatering of low-permeability sediments. *American Association of Petroleum Geologists Bulletin*, **85**, 737–48.
- Criss RE, Taylor HP Jr (1983) An $^{18}\text{O}/^{16}\text{O}$ and D/H study of Tertiary hydrothermal systems in the southern half of the Idaho batholith. *Geological Society of America Bulletin*, **94**, 640–63.
- Davidson S, Anastasio DJ, Bebout GE (1998) Volume strain associated with cleavage development in carbonate rocks, Lost River Range, Idaho. *Journal of Structural Geology*, **20**, 707–26.
- Davis D, Suppe J, Dahlen JA (1983) Mechanics of fold and thrust belts and accretionary wedges. *Journal of Geophysical Research*, **88**, 1153–72.
- Dunne WM, Hancock PL (1994) Paleostress analysis of small-scale brittle structures. In: *Continental Deformation* (ed. Hancock PL), pp. 101–20. Pergamon Press, Oxford.
- Durney DW (1972) Solution-transfer, an important geological deformation mechanism. *Nature*, **235**, 315–7.
- Eichhubl P, Taylor WL, Pollard DD, Aydin A (2004) Paleo-fluid flow and deformation in the Aztec Sandstone at the Valley of Fire, Nevada – evidence for the coupling of hydrogeologic, diagenetic, and tectonic processes. *Geological Society of America Bulletin*, **116**, 1120–36.
- Epstein AG, Epstein JB, Harris LD (1977) Conodont color alteration – an index to organic metamorphism. U.S. Geological Survey, Professional Paper 995, 27.
- Ericksen MC, Slingerland RL (1990) Numerical simulations of tidal and wind-driven circulation in the Cretaceous interior seaway of North America. *Geological Society of America Bulletin*, **102**, 1499–516.
- Evans MA, Battles DA (1999) Fluid inclusion and stable isotope analyses of veins from the central Appalachian Valley and Ridge province: implications for regional synorogenic hydrologic structure and fluid migration. *Geological Society of America Bulletin*, **111**, 1841–60.
- Evans MA, Hobbs GC (2003) Fate of ‘warm’ migrating fluids in the central Appalachians during the Late Paleozoic Alleghanian orogeny. *Journal of Geochemical Exploration*, **78–79**, 327–31.
- Ferrill DA (1991) Calcite twin widths and intensities as metamorphic indicators in natural low-temperature deformation of limestone. *Journal of Structural Geology*, **13**, 667–75.

- Fisher DM, Brantley SL (1992) Models of quartz overgrowth and vein formation: deformation and episodic fluid flow in an ancient subduction zone. *Journal of Geophysical Research*, **97**, 20043–61.
- Forster C, Smith L (1990) Chapter 1: Fluid flow in tectonic regimes. In: *Short Course on Fluids in Tectonically Active Regimes of the Continental Crust* (ed. Nesbitt BE), *Mineralogical Society of Canada Short Course Handbook Series*, **18**, 1–47.
- Garvin G, Freeze RA (1984) Theoretical Analysis of the Role of Groundwater Flow in the Genesis of Stratabound Ore Deposits. *American Journal of Science*, **284**, 1085–124.
- Ge S, Garven G (1994) A theoretical model for thrust-induced deep groundwater expulsion with application of the Canadian Rocky Mountains. *Journal of Geophysical Research*, **99**, 13851–60.
- Haley JC, Perry WJ (1990) The Red Butte conglomerate – a thrust-belt-derived conglomerate of the Beaverhead Group, southwestern Montana. U.S. Geological Survey Bulletin 1945, 19 pp., map scale 1:32,000.
- Harkins N (2002) Tectonic geomorphology of the Red Rock fault, segmentation and recent rupture history in the northern arm of the Yellowstone Topographic Wake. Masters Thesis, Lehigh University, Bethlehem, PA, 46 pp.
- Harkins NW, Latta DK, Anastasio DJ, Pazzaglia FJ (2004a) Surficial and bedrock geologic map of the Dixon Mountain 7.5' quadrangle, southwest Montana. Montana Bureau of Mines and Geology Open File Report 495, scale 1:24,000, text 12 pp., 2 pl.
- Harkins NW, Newton M, Anastasio DJ, Pazzaglia FJ (2004b) Bedrock and Surficial map of the Caboose Canyon 7.5' quadrangle, southwest Montana. Montana Bureau of Mines and Geology Open File Report 494, scale 1:24,000, text 12 pp., 2 pl.
- Henderson JR, Henderson MN, Wright TO (1990) Water-sill hypothesis for the origin of certain veins in the Meguma Group, Nova Scotia, Canada. *Geology*, **18**, 654–7.
- Holl JE, Anastasio DJ (1992) Deformation of a foreland carbonate thrust system, Sawtooth Range, Montana. *Geological Society of America Bulletin*, **104**, 944–53.
- Holl JE, Anastasio DJ (1995) Cleavage development within a foreland fold and thrust belt, Southern Pyrenees, Spain. *Journal of Structural Geology*, **17**, 357–69.
- Hubbert MK, Rubey WW (1959) Role of fluid pressure in mechanics of overthrust faulting. I. Mechanics of fluid-filled porous solids and its application to overthrust faulting. *Geological Society of America Bulletin*, **70**, 115–66.
- Hutcheon I, Cody J, Yang C (2000) Fluid flow in the Western Canada Sedimentary Basin – a biased perspective based on geochemistry. In: *Fluids and Basin Evolution*, Short Course Series, vol. 28 (ed. Keyser K), pp. ???–???. Mineralogical Association of Canada, Ottawa, ON.
- IAEA (2001) *GNIP Maps and Animations*. International Atomic Energy Agency, Vienna. <http://isohis.iaea.org>.
- Janecke SU, McIntosh W, Good S (1999) Testing models of rift basins: structure and stratigraphy of an Eocene-Oligocene supradetachment basin, Muddy Creek half graben, south-west Montana. *Basin Research*, **11**, 143–65.
- Jewell PW (1996) Circulation, salinity, and dissolved oxygen in the Cretaceous North American Seaway. *American Journal of Science*, **296**, 1093–125.
- Johnson AC (2002) Syntectonic fluid–rock interactions involving surficial fluids in the Sevier Thrust Belt, Tendoy Mountains, Southwest Montana. MS Thesis, Lehigh University, Bethlehem, PA, 120 pp.
- Kalakay TJ (2001) The role of magmatism during crustal shortening in the Sevier retroarc fold-and-thrust belt of southwest Montana. PhD Thesis, University of Wyoming, Laramie, WY.
- Kalakay TJ, John BE, Lageson DR (2001) Fault-controlled pluton emplacement in the Sevier fold-and-thrust belt of the southwest Montana, USA. *Journal of Structural Geology*, **23**, 1151–65.
- Kendall C, Sklash MMG, Bullen TD (1995) Isotope tracers of water and solute sources in catchments. In: *Solute Modeling in Catchment Systems* (ed. Trudgill ST), pp. 261–303. John Wiley & Sons, Ltd, ???.
- Koons PO, Craw D (1991) Evolution of fluid driving forces and compression within collisional orogens. *Geophysical Research Letters*, **18**, 935–8.
- Kump LR, Slingerland RL (1999) Circulation and stratification of the early Turonian Western Interior Seaway: Sensitivity to a variety of forcings. *Geological Society of America*, Special Paper, **332**, 181–90.
- Lawrence JR, Gedzelman SD (1996) Low stable isotope ratios of tropical cyclone rains. *Geophysical Research Letters*, **23**, 527–30.
- Lonn JD, Skipp B, Ruppel ET, Janecke SU, Perry WJ Jr, Sears JW, Bartholomew MJ, Stickney MC, Fritz WJ, Hurlow HA, Thomas RC (2000) *Geological Map of the Lima 30' × 60' Quadrangle, Southwest Montana*. Montana Bureau of Mines and Geology, Open File Report: MBMG 408.
- McCrea JM (1950) The isotopic chemistry of carbonated and paleotemperatures scale. *Journal of Chemical Physics*, **18**, 849–57.
- McDowell RJ (1992) Effects of synsedimentary basement tectonics on fold-thrust belt geometry, southwestern Montana. PhD Thesis, University of Kentucky, Lexington, KY.
- McDowell RJ (1997) Evidence for synchronous thin-skinned and basement deformation in the Cordilleran fold-thrust belt: the Tendoy Mountains, southwestern Montana. *Journal of Structural Geology*, **19**, 77–87.
- Nesbitt BE, Muehlenbachs K (1989) Orogens and movement of fluids during deformation and metamorphism in the Canadian Cordillera. *Science*, **245**, 733–6.
- Nesbitt BE, Muehlenbachs K (1991) Stable isotope constraints on the nature of the syntectonic fluid regime of the Canadian Cordillera. *Geophysical Research Letters*, **18**, 963–6.
- O'Neil JR, Clayton RN, Mayeda TK (1969) Oxygen isotope fractionation in divalent metal carbonates. *Journal of Chemical Physics*, **51**, 5547–58.
- Oliver J (1986) Fluids expelled tectonically from orogenic belts: their role in hydrocarbon migration and other geologic phenomena. *Geology*, **14**, 99–102.
- Oliver N, Wall V (1987) Metamorphic plumbing system in Proterozoic calc-silicates, Queensland, Australia. *Geology*, **15**, 793–6.
- Peng H, Mayer B, Harris S, Krause HR (2004) A 10-yr record of stable isotope ratios of hydrogen and oxygen in precipitation at Calgary, Alberta, Canada. *Tellus*, **56B**, 147–59.
- Perry WJ Jr, Sando WJ (1983) Sequence of deformation of Cordilleran thrust belt in Lima, Montana, region. In: *Geologic Studies of the Cordilleran Thrust Belt*, vol. 1 (ed. Powers RB), pp. 137–44, Rocky Mountain Association of Geologists, Denver, CO.
- Perry WJ, Ryder RT, Maughan EK (1981) Southern part of the Southwestern Montana thrust belt: a preliminary re-evaluation of structure, thermal maturation and petroleum potential. In: *The Montana Geological Society Field Conference and Symposium Guidebook to Southwest Montana* (eds Tucker TE, Aram RB, Brinker WF, Grabb RF Jr), pp. ???–???. Montana Geological Society, ????

- Perry WJ Jr, Wardlaw BR, Bostick NH, Maughan EK (1983) Structure, burial history, and petroleum potential of the frontal thrust belt and adjacent foreland, southwest Montana. *American Association of Petroleum Geologists Bulletin*, **67**, 725–43.
- Perry WJ Jr, Haley C, Nichols J, Hammons M, Ponton O (1988) Interactions of Rocky Mountain foreland and Cordilleran thrust belt in Lima region, southwest Montana. In: *The Interaction of Rocky Mountain Foreland and the Cordilleran Thrust Belt* (eds Schmidt CJ, Perry WJ Jr), *Geological Society of America Memoir*, **171**, ???–???
- 13 Price RA (2001) Deep refrigeration of an evolving thrust and fold belt by enhanced penetration of meteoric water: the Lewis thrust sheet, southern Canadian Rocky Mountains. *Geological Society of America, Abstracts with Programs*, vol. 33. A-52.
- 14 Ramsay JG (1980) The crack-seal mechanism of rock deformation. *Nature*, **284**, 135–9.
- Roedder E (1984) *Fluid Inclusions (Rev. Mineral., vol. 12)*. Mineralogical Society of America, Washington, D.C., 644 pp.
- Rolland Y, Cox S, Bollier A-M, Pennacchioni G, Mancktelow N (2003) Rare earth and trace element mobility in mid-crustal shear zones: insight from the Mont Blanc Massif (Western Alps). *Earth and Planetary Science Letters*, **214**, 203–19.
- 15 Rye DM, Bradbury HJ (1988) Fluid flow in the crust: an example from a Pyrenean thrust ramp. *American Journal of Science*, **288**, 197–235.
- Sageman BB (1996) Lowstand tempestites: depositional model for Cretaceous skeletal limestones, Western Interior basin. *Geology*, **24**, 888–92.
- Schmitt JG, Haley JC, Lageson DR, Horton BK, Azevedo PA (1995) Sedimentology and tectonics of the Bannack-McKnight Canyon-Red Butte Area, southwest Montana: new perspectives on the Beaverhead Group and Sevier Orogenic Belt. *Northwest Geology*, **24**, 245–313.
- 16 17 Scotese C (2002) *Paleogeographic maps*. <http://www.scotese.com>.
- Sheppard SMF (1996) Characterization and isotopic variations in natural waters. In: *Stable Isotopes in High-temperature Geological Processes* (eds Valley JW, Taylor HP Jr, O'Neil JR). *Reviews in Mineralogy*, **16**, 165–83.
- Sheppard SMF, Nielsen RL, Taylor HP Jr (1969) Oxygen and hydrogen isotope ratios of clay minerals from porphyry copper deposits. *Economic Geology*, **64**, 755–77.
- 18 Siegenthaler W (1979) Stable hydrogen and oxygen isotopes in the water cycle. In: *Lectures in Isotope Geology* (eds Jaeger E, Hunziker JC). pp. ???–???, Springer-Verlag, Berlin.
- 19 Skipp B (1988) Cordilleran thrust belt and faulted foreland in the Beaverhead Mountains, Idaho and Montana. In: *The Interaction of Rocky Mountain Foreland and the Cordilleran Thrust Belt* (eds Schmidt CJ, Perry WJ Jr), *Geological Society of America, Memoir* 171, ???–???
- 20 Slingerland R, Kump LR, Arthur MA, Fawcett PJ, Sageman BB, Barron EJ (1996) Estuarine circulation in the Turonian Western Interior Seaway of North America. *Geological Society of America Bulletin*, **108**, 941–52.
- Sterns DW (1969) Fracture as a mechanism of flow in naturally deformed layered rocks. *Geological Survey of Canada Special Paper*, **68-52**, 79–95.
- 21 Suppe J, Wittke JH (1977) Abnormal pore-fluid pressures in relation to stratigraphy and structure in the active fold-and-thrust belt in northwestern Taiwan. *Petroleum Geology of Taiwan*, **14**, 11–24.
- Swetland PJ, Clayton JL, Sable EG (1978) Petroleum source-bed potential of Mississippian-Pennsylvanian rocks in parts of Montana, Idaho, Utah, and Colorado. *Mountain Geology*, **14**, 79–87.
- Tavernelli E (1997) Structural evolution of a foreland fold-and-thrust belt: the Umbria-Marche Apennines, Italy. *Journal of Structural Geology*, **19**, 523–34.
- Whittaker SG, Keyser TK, Caldwell WGE (1987) Paleoenvironmental geochemistry of the Claggett marine cyclothem in south-central Saskatchewan. *Canadian Journal of Earth Science*, **24**, 967–84.
- Wojtal S (1986) Deformation within foreland thrust sheets by populations of minor faults. *Journal of Structural Geology*, **11**, 669–78.
- 22 Yurtsever Y, Gat JR (1981) Atmospheric water. In: *Stable Isotope Hydrology, Deuterium and Oxygen-18 in the Water Cycle, Vienna* (ed. ??? ?), pp. 103–42. International Atomic Energy Agency, Vienna.
- 23

Author Query Form

Journal: GFL

Article: 146

Dear Author,

During the copy-editing of your paper, the following queries arose. Please respond to these by marking up your proofs with the necessary changes/additions. Please write your answers on the query sheet if there is insufficient space on the page proofs. Please write clearly and follow the conventions shown on the attached corrections sheet. If returning the proof by fax do not write too close to the paper's edge. Please remember that illegible mark-ups may delay publication.

Many thanks for your assistance.

Query reference	Query	Remarks
1	Author: please provide telephone and fax numbers.	
2	Production Editor: please supply dates.	
3	Author: please supply up to six keywords for indexing.	
4	Author: please provide page range.	
5	Author: please provide the publisher and place of publication.	
6	Author: Garvin, Freeze (1984) not cited. Please cite reference in text or delete from the list.	
7	Author: please provide page range.	
8	Author: please check this website address, confirm that it is correct, and provide the date of last access.	
9	Author: please check volume number.	
10	Author: Johnson (2002) not cited. Please cite reference in text or delete from the list.	
11	Author: please provide the place of publication.	
12	Author: please provide page range and place of publication.	
13	Author: please provide page range.	
14	Author: Ramsay (1980) not cited. Please cite reference in text or delete from the list.	
15	Author: Rolland, Cox, Bollier, Pennacchioni, Mancktelow (2003) not cited. Please cite reference in text or delete from the list.	
16	Author: Schmitt, Haley, Lageson, Horton, Azevedo (1995) not cited. Please cite reference in text or delete from the list.	
17	Author: please check this website address, confirm that it is correct, and provide the date of last access.	

18	Author: Sheppard, Nielsen, Taylor (1969) not cited. Please cite reference in text or delete from the list.	
19	Author: please provide page range.	
20	Author: please provide page range.	
21	Author: please check volume number.	
22	Author: Wojtal (1986) not cited. Please cite reference in text or delete from the list.	
23	Author: please provide the Editors for this book and check place of publication.	

MARKED PROOF

Please correct and return this set

Please use the proof correction marks shown below for all alterations and corrections. If you wish to return your proof by fax you should ensure that all amendments are written clearly in dark ink and are made well within the page margins.

<i>Instruction to printer</i>	<i>Textual mark</i>	<i>Marginal mark</i>
Leave unchanged	... under matter to remain	Stet
Insert in text the matter indicated in the margin	⤴	New matter followed by ⤴
Delete	⤵ through matter to be deleted	⤵
Delete and close up	⤵ through matter to be deleted	⤵
Substitute character or substitute part of one or more word(s)	/ through letter or ⤵ through word	New letter or new word
Change to italics	— under matter to be changed	≡
Change to capitals	≡ under matter to be changed	≡
Change to small capitals	≡ under matter to be changed	≡
Change to bold type	⤵ under matter to be changed	⤵
Change to bold italic	⤵ under matter to be changed	⤵
Change to lower case	Encircle matter to be changed	⊖
Change italic to upright type	(As above)	⤴
Insert 'superior' character	/ through character or ⤴ where required	⤴ under character e.g. ⤴
Insert 'inferior' character	(As above)	⤵ over character e.g. ⤵
Insert full stop	(As above)	⦿
Insert comma	(As above)	,
Insert single quotation marks	(As above)	⤴ and/or ⤵
Insert double quotation marks	(As above)	⤴ and/or ⤵
Insert hyphen	(As above)	Ⓜ
Start new paragraph	⤴	⤴
No new paragraph	⤵	⤵
Transpose	⤴	⤴
Close up	linking ⦿ letters	⦿
Insert space between letters	⤴ between letters affected	#
Insert space between words	⤴ between words affected	#
Reduce space between letters	⤴ between letters affected	⤴
Reduce space between words	⤴ between words affected	⤴